Title:

A novel non-terminal tumor sampling procedure using fine needle aspiration supports immune-oncology biomarker discovery in preclinical mouse models

Supplementary figures and figure legends:

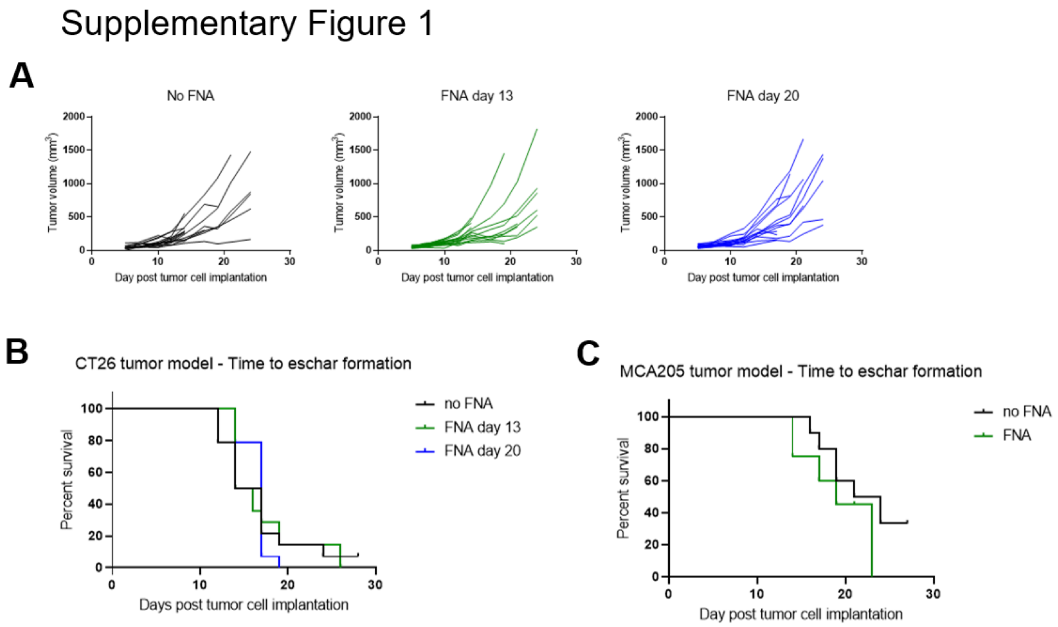

Supplementary Figure 1: Fine needle aspiration does not impact tumor growth or eschar formation

(**A** and **B**) Mice were subcutaneously implanted with CT26 tumors on the flank and the tumors were biopsied using FNA either 13 or 20 days later. (**A**) Tumor growth of individual mice over time. (**B**) Time to eschar formation was compared between groups using a log-rank test. No significant differences were seen between FNA-biopsied and control groups. (**C**) Mice were subcutaneously implanted with MCA205 tumors on the flank and the tumors were biopsied using FNA 18 days later. Time to eschar formation was compared between groups using a log-rank test. No significant differences were seen between FNA-biopsied and control groups.

Supplementary Figure 2

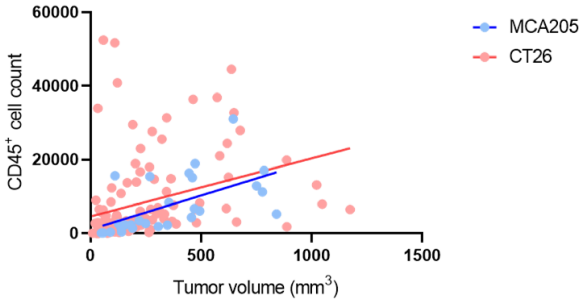

Supplementary Figure 2: Fine needle aspiration can be used to extract cells for flow cytometry at a range of tumor volumes

FNA biopsies were collected from mice bearing either CT26 or MCA205 tumors and analysed by flow cytometry to determine the total number of $CD45^+$ tumor-infiltrating immune cells within the sample. This was plotted against the volume of the tumor on the day of FNA biopsying for each mouse and linear regression was used to calculate the correlation between the $CD45^+$ cell count and tumor volume for both tumor models, indicated by the solid lines. 27-124 mice per group.

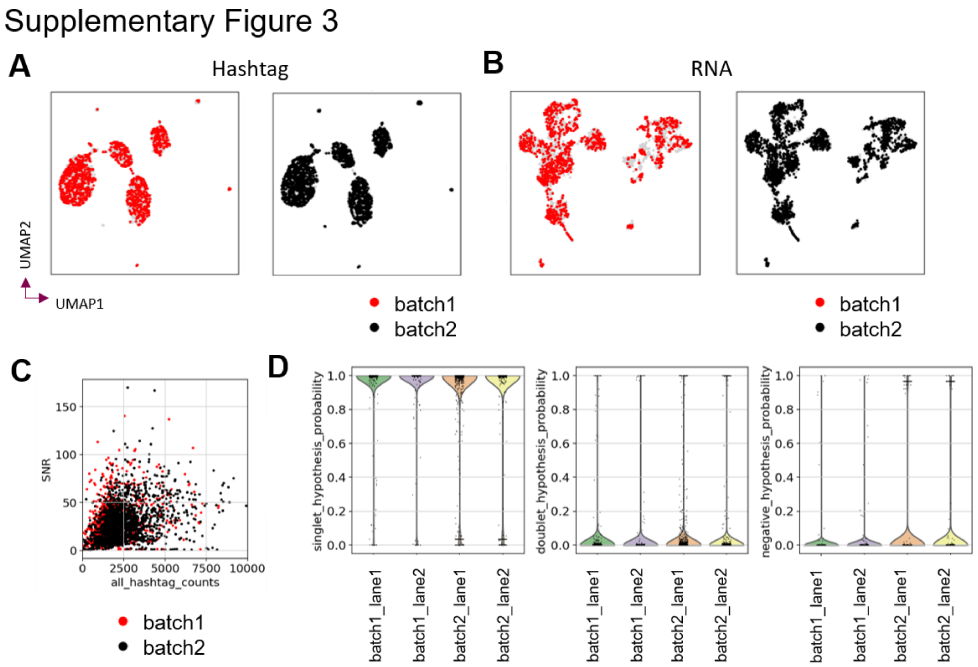

Supplementary Figure 3: Optimising single cell RNA sequencing parameters for use with fine needle aspiration samples

(**A**) Hashtag-embedded UMAP colored by batch. (**B**) RNA-embedded UMAPs colored by batch. (**C**) Number of hashtag counts per cell versus Signal-Noise Ratio (SNR) per cell. SNR was calculated for each cell as the most frequent hashtag count divided by all other hashtag counts. (**D**) Comparison of hashsolo probabilities of singlet, doublet/multiplet or negative assignment across the different batches and lanes.

Supplementary Figure 4

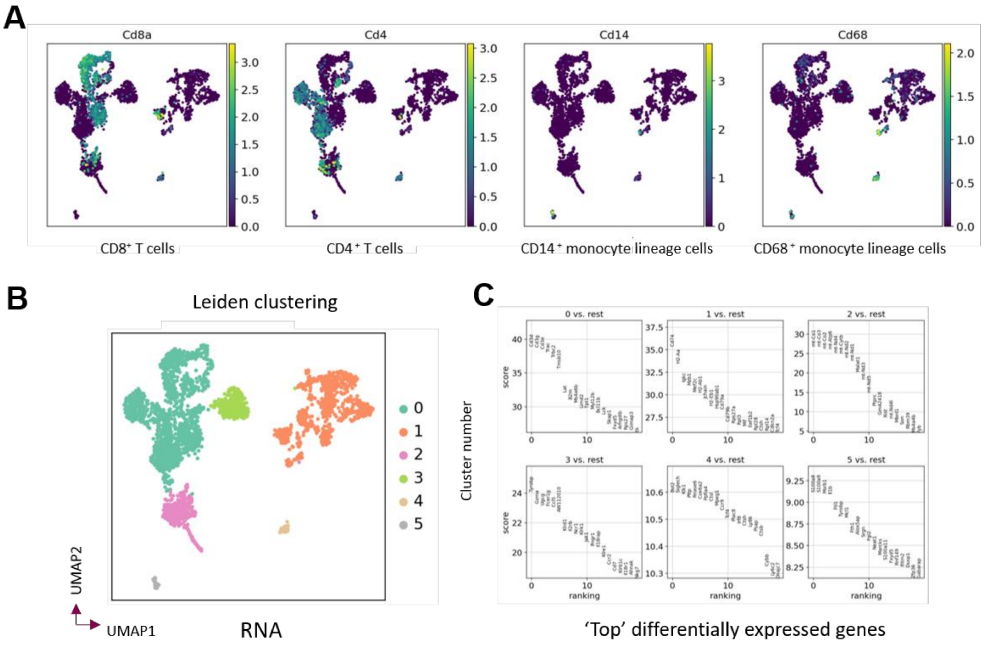

Supplementary Figure 4: Fine needle aspiration enables single cell RNA sequencing

Expression of putative marker genes of immune cell types. (**B**) RNA UMAP colored by clustering annotation. (**C**) Top ranked (based on Z-score) differentially expressed genes between each cluster versus all other clusters.

Supplementary Figure 5

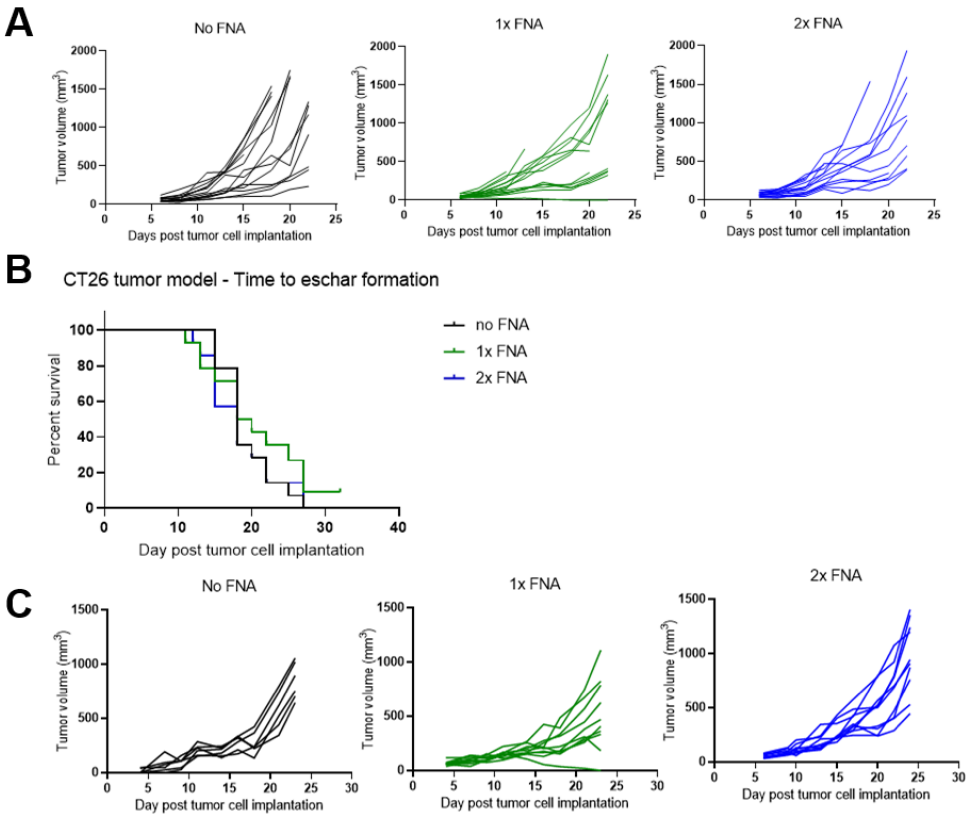

Supplementary Figure 5: Repeated fine needle aspiration does not impact tumor growth or eschar formation

(**A** and **B**) Mice were subcutaneously implanted with CT26 tumors on the flank and the tumors were biopsied using FNA either 12 days later (1x FNA group) or 12 and 14 days later (2x FNA group). (**A**) Tumor growth of individual mice over time. (**B**) Time to eschar formation was compared between groups using a log-rank test. No significant differences were seen between FNA-biopsied and control groups. (**C**) Mice were subcutaneously implanted with A20 tumors on the flank and the tumors were sampled using FNA either 15 days later (1x FNA group) or 13 and 15 days later (2x FNA group). Tumor growth of individual mice over time.

Supplementary Figure 6

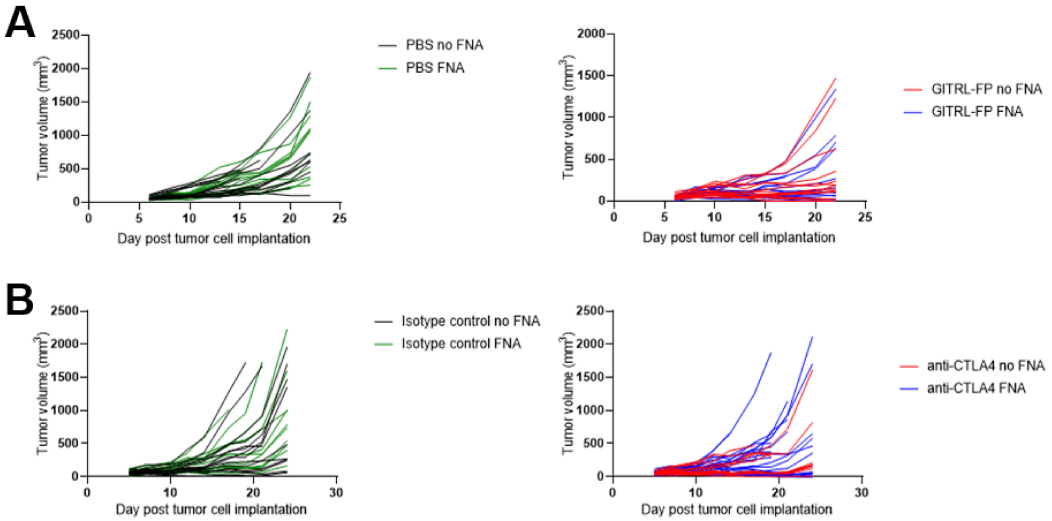

Supplementary Figure 6: Fine needle aspiration does not affect response to immuno-oncology treatments

(**A**) CT26 tumor-bearing mice were treated with 0.2mg/kg GITRL-FP on day 6 and half of the mice were biopsied using FNA on day 14. Tumor growth of individual mice over time. (**B**) CT26 tumor-bearing mice were treated with 10mg/kg anti-CTLA-4 antibody or isotype control twice weekly from day 7 for 6 doses and half of the mice were biopsied using FNA on day 14. Tumor growth of individual mice over time.

Supplementary Figure 7

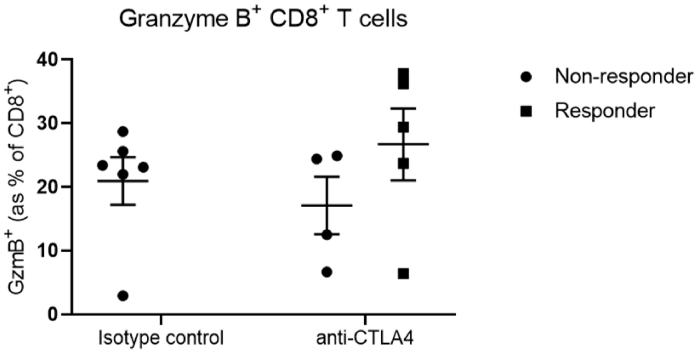

Supplementary Figure 7: Fine needle aspiration enables intracellular cytokine staining

CT26 tumor-bearing mice were treated with 10mg/kg anti-CTLA-4 antibody or isotype control twice weekly from day 7 for 6 doses and the tumors were biopsied using FNA on day 17. Flow cytometric analysis of the FNA biopsies was used to quantify the frequency of Granzyme B-expressing $CD8^+$ T cells after subdividing the treated group into responder and non-responder groups *post hoc* based on the outcome of the tumor growth inhibition study.

Supplementary Figure 8

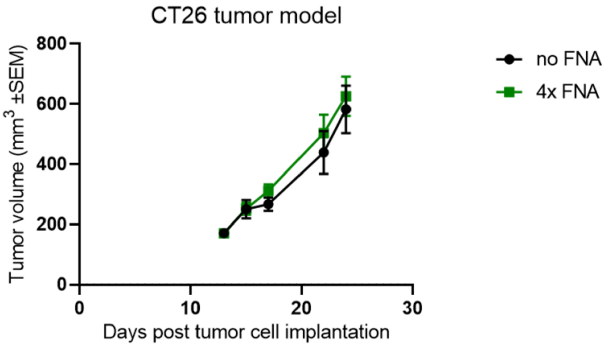

Supplementary Figure 8: Fine needle aspiration can be carried out four times without impacting tumor growth

Mice were subcutaneously implanted with CT26 tumors on the flank and the tumors were biopsied using FNA 12, 15, 18 and 21 days later (4x FNA group). Tumor growth over time was compared between groups using a mixed effects model. No significant differences were seen between FNA-biopsied and control groups. Error bars indicate the mean ± SEM. 10 mice per group.

Supplementary Figure 9

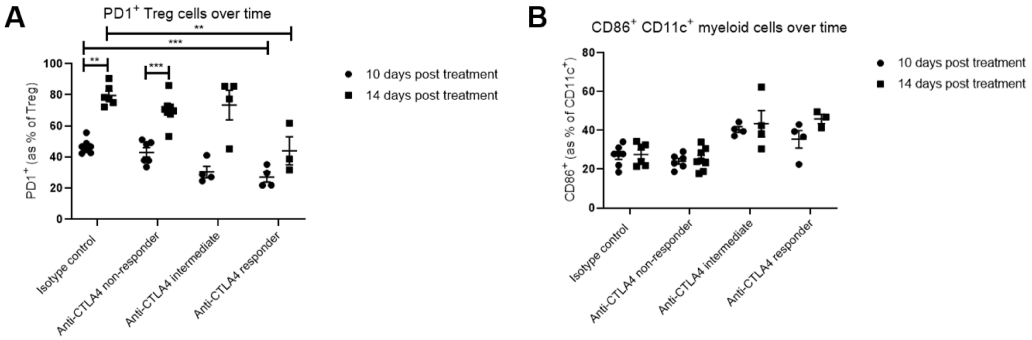

Supplementary Figure 9: Repeated fine needle aspiration enables comparison of the TME at several timepoints after treatment

CT26 tumor-bearing mice were treated with 10mg/kg anti-CTLA-4 antibody or isotype control twice weekly from day 7 for 6 doses and the tumors were biopsied using FNA on day 17 (10 days post treatment initiation) and day 21 (14 days post treatment initiation). Flow cytometric analysis of the FNA biopsies was used to compare (**A**) the frequency of PD1-expressing Treg cells and (**B**) the frequency of CD86-expressing $CD11c^+$ myeloid cells after subdividing the treated group into responder, intermediate and non-responder groups *post hoc* based on the outcome of the tumor growth inhibition study. The 2 timepoints were compared using Mann-Whitney tests with multiple comparison correction. For each timepoint, the treatment groups were compared using a one-way ANOVA with Tukey's multiple comparison testing. Error bars indicate the mean ± SEM. ** $P < 0.01$, *** $P < 0.001$.

A

Batch	Library Type	Estimated Number of Cells	Mean Reads per Cell	Median Genes per Cell	Number of Reads	Valid Barcodes	Sequencing Saturation	Q30 Bases in Barcode	Q30 Bases in RNA Read	Q30 Bases in Sample Index	Q30 Bases in UMI	Reads Mapped to Genome	Reads Mapped Confidently to Genome	Reads Mapped Confidently to Intergenic Regions	Reads Mapped Confidently to Intronic Regions	Reads Mapped Confidently to Exonic Regions	Reads Mapped Confidently to Transcriptome	Reads Mapped Antisense to Gene	Fraction Reads in Cells	Total Genes Detected	Median UMI Counts per Cell
1	RNA	1,098	371,898	1,915	408,344,185	97.80%	94.10%	95.70%	93.50%	95.70%	94.90%	91.10%	84.90%	4.00%	21.40%	59.50%	56.80%	1.20%	86.20%	16,742	5,296
2	RNA	2,053	101,129	1,933	207,618,619	97.70%	79.40%	95.70%	93.60%	96.10%	94.90%	92.20%	86.40%	3.80%	21.80%	60.70%	58.00%	1.10%	88.10%	17,467	5,269

B

Batch	Library Type	Number of Reads	Mean Reads per Cell	Valid Barcodes	Sequencing Saturation	Q30 Bases in Barcode	Q30 Bases in Antibody Read	Q30 Bases in Sample Index	Q30 Bases in UMI	Fraction Antibody Reads	Fraction Antibody Reads Usable	Antibody Reads Usable per Cell	Fraction Reads in Barcodes with High UMI Counts	Fraction Unrecognized Antibody	Antibody Reads in Cells	Median UMIs per Cell (summed over all recognized antibody barcodes)
1	Antibody	7,116,195	6,481	99.10%	51.50%	96.10%	96.00%	90.80%	96.30%	87.30%	58.00%	3,759	0.00%	12.70%	66.80%	1,586
2	Antibody	16,431,509	8,003	99.10%	57.10%	96.00%	96.00%	91.30%	96.20%	91.30%	69.20%	5,539	0.00%	8.70%	76.20%	2,072

Supplementary Table 1: QC metrics for scRNAseq per batch

Quality control metrics from cellranger count for each batch for (**A**) RNA and (**B**) antibody hashtag.

A

Batch	Lane	Library Type	Estimated Number of Cells	Mean Reads per Cell	Median Genes per Cell	Number of Reads	Valid Barcodes	Sequencing Saturation	Q30 Bases in Barcode	Q30 Bases in RNA Read	Q30 Bases in Sample Index	Q30 Bases in UMI	Reads Mapped to Genome	Reads Mapped Confidently to Genome	Reads Mapped Confidently to Intergenic Regions	Reads Mapped Confidently to Intronic Regions	Reads Mapped Confidently to Exonic Regions	Reads Mapped Confidently to Transcriptome	Reads Mapped Antisense to Gene	Fraction Reads in Cells	Total Genes Detected	Median UMI Counts per Cell
1	1	RNA	1,076	184,313	1,863	198,321,366	97.80%	88.80%	95.90%	93.70%	95.90%	95.00%	91.10%	84.90%	4.00%	21.30%	59.60%	56.90%	1.20%	86.10%	16,448	5,133
1	2	RNA	1,075	195,370	1,870	210,022,819	97.70%	89.40%	95.60%	93.30%	95.50%	94.70%	91.10%	85.00%	4.00%	21.40%	59.50%	56.80%	1.20%	86.20%	16,479	5,153
2	1	RNA	1,943	52,460	1,757	101,931,446	97.70%	65.20%	95.80%	93.80%	96.30%	95.00%	92.20%	86.40%	3.80%	21.70%	60.80%	58.00%	1.10%	88.00%	16,954	4,681
2	2	RNA	1,937	54,562	1,780	105,687,173	97.70%	66.00%	95.50%	93.40%	95.90%	94.70%	92.20%	86.40%	3.80%	21.80%	60.70%	57.90%	1.20%	88.10%	17,001	4,732

B

Batch	Lane	Library Type	Number of Reads	Mean Reads per Cell	Valid Barcodes	Sequencing Saturation	Q30 Bases in Barcode	Q30 Bases in Antibody Read	Q30 Bases in Sample Index	Q30 Bases in UMI	Fraction Antibody Reads	Fraction Antibody Reads Usable	Antibody Reads Usable per Cell	Fraction Reads in Barcodes with High UMI Counts	Fraction Unrecognized Antibody	Antibody Reads in Cells	Median UMIs per Cell (summed over all recognized antibody barcodes)
1	1	Antibody	4,942,840	4,593	99.10%	42.70%	96.20%	96.00%	91.00%	96.40%	87.30%	57.90%	2,661	0.00%	12.70%	66.80%	1,309
1	2	Antibody	2,173,355	2,021	99.00%	26.90%	95.90%	95.90%	90.40%	96.10%	87.40%	58.00%	1,172	0.00%	12.60%	66.80%	724
2	1	Antibody	11,179,458	5,753	99.10%	47.40%	96.10%	96.00%	91.50%	96.30%	91.30%	68.60%	3,945	0.00%	8.70%	75.60%	1,765
2	2	Antibody	5,252,051	2,711	99.10%	31.00%	95.80%	96.00%	91.00%	96.10%	91.40%	68.70%	1,863	0.00%	8.60%	75.70%	1,083

Supplementary Table 2: QC metrics for scRNAseq per lane

Quality control metrics from cellranger count for each batch split by lane for (**A**) RNA and (**B**) antibody hashtag.